
SUPPORTING INFORMATION

Reversible Dispersion and Release of Carbon Nanotubes via Cooperative Clamping Interactions with Hydrogen-bonded Nanorings

Raquel Chamorro,^a Leire de Juan-Fernández,^b Belén Nieto-Ortega,^b Maria J. Mayoral,^a Santiago Casado,^b Luisa Ruiz-González,^c Emilio M. Pérez*^b and David González-Rodríguez*^{a,d}

^a Organic Chemistry Department, Universidad Autónoma de Madrid, 28049 Madrid, Spain.
E-mail: david.gonzalez.rodriguez@uam.es

^b IMDEA Nanociencia, c/Faraday 9, Campus de Cantoblanco, 28049, Madrid, Spain.
E-mail: emilio.perez@imdea.org

^c Inorganic Chemistry Department, Universidad Complutense de Madrid, 28040, Madrid, Spain.

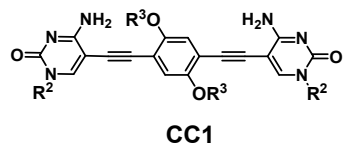
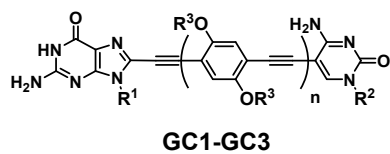
^d Institute for Advanced Research in Chemical Sciences (IAdChem), Universidad Autónoma de Madrid, 28049 Madrid

SUPPORTING INFORMATION

TABLE OF CONTENTS

S1. Monomer structure	2
S2. Synthesis and Characterization	3
S3. Preliminary study of the self-assembly behavior of GC1	14
S4. Characterization of the pristine (6,5)-enriched SWNTs	16
S5. Computational Details	17
S6. Characterization of the CNT-GC1 conjugates by HR-TEM	19
S7. Dilution experiments monitored by fluorescence spectroscopy	20
S8. References	21

S1. Monomer structure



	R^1	R^2	R^3
GC1 (n=1)			C_4H_7
GC2 (n=1)			C_4H_7
GC3 (n=0)	C_2H_5		
CC1 (n=1)			C_4H_7

S2. Synthesis and Characterization

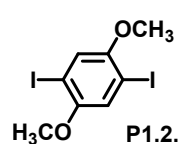
General Methods. Mass Spectrometry (MS) and High Resolution-Mass Spectrometry (HRMS) spectra were measured on a VG AutoSpec apparatus (FAB) or an *Applied Biosystems QSTAR* equipment (ESI) in the positive or negative modes. MALDI-TOF spectra were obtained from a BRUKER ULTRAFELEX III instrument equipped with a nitrogen laser operating at 337 nm. **NMR** spectra were recorded with a *BRUKER AVANCE-II* (300 MHz) instrument. The temperature was actively controlled at 298 K. Chemical shifts are measured in ppm using the signals of the deuterated solvent as the internal standard [CDCl_3 calibrated at 7.26 ppm (^1H) and 75.0 ppm (^{13}C), DMSO-d_6 calibrated at 2.50 ppm (^1H) and 39.5 ppm (^{13}C) and THF-d_8 calibrated at 3.58 (^1H)]. **Column chromatography** was carried out on silica gel *Merck-60* (230-400 mesh, 60 Å), and TLC on aluminium sheets precoated with silica gel 60 F254 (Merck). **UV-Visible** experiments were conducted using a *JASCO V-660* apparatus. **Emission spectra** were recorded in a *JASCO FP-8600* equipment using excitation and emission bandwidths of 5 nm in both cases, and a 50 ms response. **CD spectra** were recorded with a *JASCO V-815* equipment. The slit width was set at 1000 μm and a DIT of 2 s was used. In all these three instruments the temperature was controlled using a *JASCO* Peltier thermostatted cell holder with a range of 263–383 K, adjustable temperature slope, and accuracy of ± 0.1 K. **Raman** spectra were acquired with a *Bruker Senterra* confocal Raman microscopy instrument, equipped with 532, 633 and 785 nm lasers. **Termogravimetric analyses (TGA)** were performed using a *TA Instruments TGAQ500* with a ramp of 50 $^\circ\text{C}/\text{min}$ under air from 100 to 1000 $^\circ\text{C}$. **Transmission electron microscopy (TEM)** images were obtained with a *JEOL-JEM 2100F* (2.5 Å resolution) instrument operating at 200 kV. **Aberration corrected HR-TEM** images were obtained with a *GRAND ARM300cf JEOL* instrument operating at 60 kV. **Atomic force microscopy (AFM)** images were obtained with *JPK NanoWizard II instrument*, coupled to an inverted optical microscope *Nikon Eclipse Ti-U*.

Starting materials. Chemicals were purchased from commercial suppliers and used without further purification. Solid hygroscopic reagents were dried in a vacuum oven before use. Reaction solvents were thoroughly dried before use using standard methods. Monomers **GC2** and **GC3** were synthesized previously.^{S1,S2} The complete synthetic routes to monomers **GC1** and **CC1**, as well as the characterization of all final and intermediate compounds, is detailed below.

Synthetic procedures and characterization data for P1.

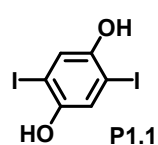


Scheme S1. Synthetic route to **P1**.



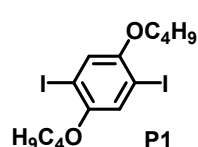
P1.2. was obtained following a previously reported synthetic route.^{S3} Iodine (90.08 mmol, 22.86 g) was added to a suspension of H_5IO_6 (111.36 mmol, 25.40 g) in MeOH (50 mL) at room temperature. After 10 min, a solution of 1,4-dimethoxybenzene (70.9 mmol, 10 g) in the minimum volume of MeOH possible was added. The reaction mixture was stirred at 70 °C for 4 h. After completion, the reaction mixture was let to cool down to room temperature and a turbid solution was obtained because of the formation of a precipitate by the addition of $\text{Na}_2\text{S}_2\text{O}_5$ (sat.). The precipitate was filtered and washed with MeOH. Then the precipitate was dissolved in CH_2Cl_2 and evaporated *in vacuo*. **P1.2.** was obtained as a white solid (24.0 g, 87 %).

$^1\text{H NMR}$ (300 MHz, CDCl_3) δ (ppm) = 7.19 (s, 2H, Ar-H), 3.83 (s, 6H, $-\text{CH}_3$)



P1.1. was obtained following the indicated procedure.^{S4} A solution of BBr_3 in CH_2Cl_2 (56.4 mmol, 56.4 mL, 1M) was added dropwise to a solution of **P1.2.** (25.64 mmol, 10 g) in CH_2Cl_2 (150 mL) at 0 °C. The reaction mixture was stirred 24 h at room temperature. Then, water was carefully added over the mixture at 0 °C and the resulting precipitate was filtered and washed with water. **P1.1.** was obtained as a white solid (9.10 g, 98 %).

$^1\text{H NMR}$ (300 MHz, CDCl_3) δ (ppm) = 7.29 (s, 2H, Ar-H), 4.98 (s, 2H, $-\text{OH}$)

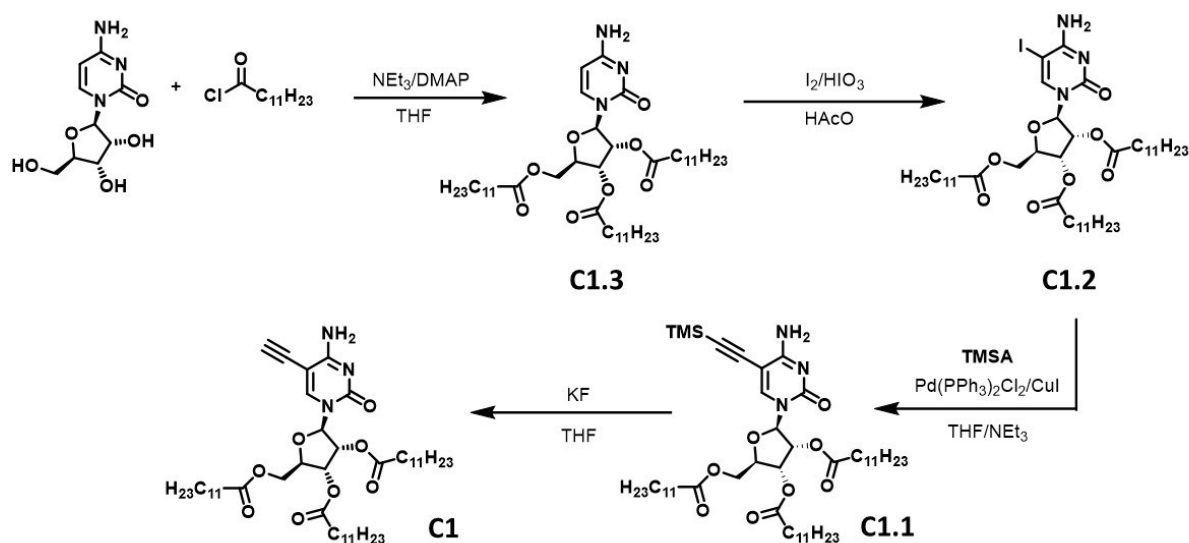


P1. The synthesis of **P1** has been previously reported.^{S5} 1-bromobutane (121 mmol, 13.05 g) was added dropwise over a solution of **P1.2.** (55.26 mmol, 20 g) and KOH (166 mmol, 9.30 g) in dry DMF (200 mL) at 0 °C and stirred overnight. After reaction completion the solvent was evaporated and the resulting residue was washed three times with $i\text{Pr}_2\text{O}$, then with HCl 0.1M and finally dried with MgSO_4 . The resulting crude was purified by column chromatography using cyclohexane/DCM (4:1) as eluents. **P1** was obtained as a white solid (23 g, 89 %).

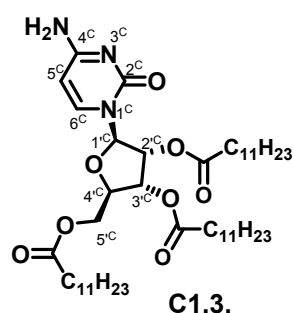
$^1\text{H NMR}$ (300 MHz, CDCl_3) δ (ppm) = 7.18 (s, 2H, Ar-H), 3.93 (t, J = 6.0 Hz, 4H, OCH_2-), 1.83-1.74 (m, 4H, OCH_2CH_2-), 1.60-1.47 (m, 4H, $-\text{CH}_2-\text{CH}_3$), 0.98 (t, J = 7.0 Hz, 6H, $-\text{CH}_3$).

$^{13}\text{C NMR}$ (76 MHz, CDCl_3) δ (ppm) = 152.8, 122.7, 86.3, 70.0, 31.2, 19.3, 13.8

Synthetic procedures and characterization data for C1.



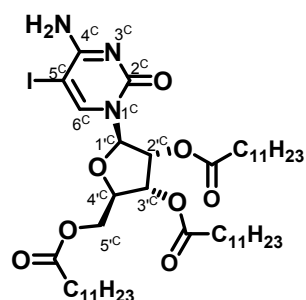
Scheme S2. Synthetic route to C1.



C1.3. In a 1000 mL round-bottomed flask (equipped with a magnetic stirrer), commercial cytidine (41.1 mmol, 10 g) and DMAP (8.2 mmol, 1.01 g) were dissolved in dry THF (250 mL). NEt₃ (184.5 mmol, 25.8 mL) was added and the mixture was cooled at 0 °C. Lauroyl chloride (127.5 mmol, 9.4 mL) was then added dropwise and the mixture stirred at room temperature under argon during 12h. The solvent was eliminated under reduced pressure and the oil residue was dissolved in AcOEt and successively washed with NaHCO₃ (sat.) and H₂O (3 x 150 mL). The organic layer was dry over Na₂SO₄, filtered and the solvent evaporated *in vacuum* to dryness. The residue was finally purified by chromatography on silica gel eluted with cyclohexane/AcOEt (6:1). **C1.3.** was obtained as a yellow solid (18 g, 56 %).

¹H NMR (300 MHz, CDCl₃) δ(ppm) = 9.24 (s, 1H, NH^{4c}), 7.89 (d, *J* = 7.5 Hz, 1H, H^{6c}), 7.47 (d, *J* = 7.5 Hz, 1H, H^{5c}), 6.10 (d, *J* = 4.0 Hz, 1H, H^{7c}), 5.72 (s, 1H, NH^{4c}), 5.39 (dd, *J* = 5.5, 4.0 Hz, 1H, H^{2c}), 5.30 (dd, *J* = 7.0, 4.0 Hz, 1H, H^{4c}), 4.44-4.26 (m, 3H, CH₂^{5c}, H^{3c}), 2.46-2.81 (m, 6H, -OCOCH₂-), 1.75-1.48 (m, 6H, OCOCH₂CH₂-), 1.26 (m, 48H, OCOC₂H₄-(CH₂)_{*n*}-), 0.95-0.76 (m, 9H -CH₃).

¹³C NMR (75 MHz, CDCl₃) δ(ppm) = 173.0, 172.2, 172.1, 162.9, 154.8, 143.8, 97.1, 89.1, 80.0, 73.7, 69.5, 62.6, 37.7, 34.1, 33.8, 31.9, 29.6, 29.5, 29.4, 29.3, 29.1, 24.9, 24.8, 24.7, 22.7, 14.1.



C1.2. I₂ (5.7 mmol, 1.45 g) and HIO₃ (5.7 mmol, 1 g) were added over a solution of **C1.3.** (5.19 mmol, 4.10 g) in acetic acid (40 mL). The solution was stirred at 40 °C and followed by TLC. Once completed, the reaction mixture was cooled, the excess of HIO₃ filtered, and the solution extracted with AcOEt/Et₂O (1:1), and washed with water, NaHCO₃ (sat.) and Na₂S₂O₃ (sat.). The organic layer was then dry with Na₂SO₄, filtered and concentrated *in*

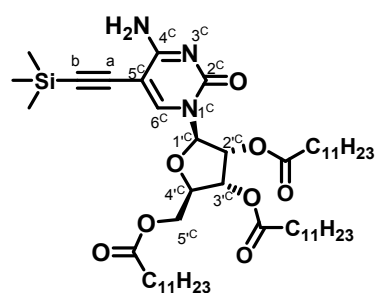
C1.2.

vacuo. The final residue was purified by column chromatography on silica gel eluted with cyclohexane/AcOEt (4:1) affording **C1.2**. (1.10 g, 23 %) as a yellow oil.

¹H NMR (300 MHz, CDCl₃) δ(ppm) = 9.05 (s, 1H, NH^{4c}), 7.85 (s, 1H, H^{6c}), 6.05 (d, *J* = 4.0 Hz, 1H, H^{1c}), 5.73 (s, 1H, NH^{4c}), 5.49-5.13 (m, 2H, H^{2c}, H^{4c}), 4.42-4.26 (m, 3H, CH₂^{5c}, H^{3c}), 2.44-2.19 (m, 6H, -OCOCH₂-), 1.61 (m, 6H, OCOCH₂CH₂-), 1.23 (m, 48H, OCOC₂H₄-(CH₂)_{*n*}-) 0.94-0.78 (m, 9H, -CH₃).

¹³C NMR (75 MHz, CDCl₃) δ(ppm) = 173.1, 172.3, 172.2, 163.8, 154.3, 146.2, 88.3, 79.8, 73.6, 69.4, 62.5, 57.6, 37.3, 35.4, 34.3, 33.9, 33.8, 33.4, 29.6, 29.5, 29.5, 29.4, 29.3, 29.1, 25.2, 24.8, 24.7, 22.7, 14.1.

HRMS (ESI+): Calculated for C₄₅H₇₉IN₃O₈: 916.4834 [M+H]⁺. Found: 916.4984.



C1.1.

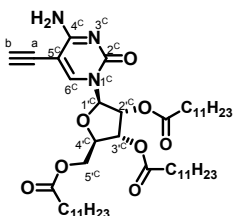
C1.1. A dry THF/NEt₃ (4:1) solvent mixture was subjected to deoxygenation by three *freeze-pump-thaw* cycles with argon. Then, this solvent was added over the system containing **C1.2**. (2.89 mmol, 2.65 g), Pd(PPh₃)₂Cl₂ (0.06 mmol, 40 mg) and CuI (0.02 mmol, 6 mg). The mixture was stirred at room temperature during a few minutes. Then, trimethylsilylacetylene (8.7 mmol, 1.2 mL) was added dropwise. The reaction was stirred at 40 °C for 24 h until completion. Then, the mixture was filtered over celite and the solvent evaporated under vacuum. The

crude was purified by column chromatography with cyclohexane/AcOEt (4:1). The product **C1.1** was obtained as yellow oil (2.17 g, 85 %)

¹H NMR (300 MHz, CDCl₃) δ(ppm) = 8.62 (s, 1H, NH^{4c}), 7.78 (s, 1H, H^{6c}), 6.12 (d, *J* = 4.0 Hz, 1H, H^{1c}), 5.84 (s, 1H, NH^{4c}), 5.43-5.21 (m, 2H, H^{2c}, H^{4c}), 4.43-4.28 (m, 3H, CH₂^{5c}, H^{3c}), 2.48-2.23 (m, 6H, OCOCH₂-), 1.70-1.52 (m, 6H, OCOCH₂CH₂-), 1.26 (m, 48H, OCOC₂H₄-(CH₂)_{*n*}-), 0.95-0.79 (m, 9H, -CH₃), 0.22 (s, 9H, (CH₃)₃Si).

¹³C NMR (75 MHz, CDCl₃) δ(ppm) = 173.4, 173.1, 172.4, 172.4, 167.7, 153.9, 143.6, 101.9, 95.5, 92.5, 88.3, 79.8, 73.8, 69.6, 62.7, 37.4, 35.5, 34.2, 34.0, 33.9, 33.5, 32.0, 29.7, 29.7, 29.7, 29.6, 29.6, 29.5, 29.4, 29.3, 29.2, 25.3, 25.0, 24.9, 22.8, 14.2.

MS (FAB+): found: 886.6 [M+H]⁺.



c1

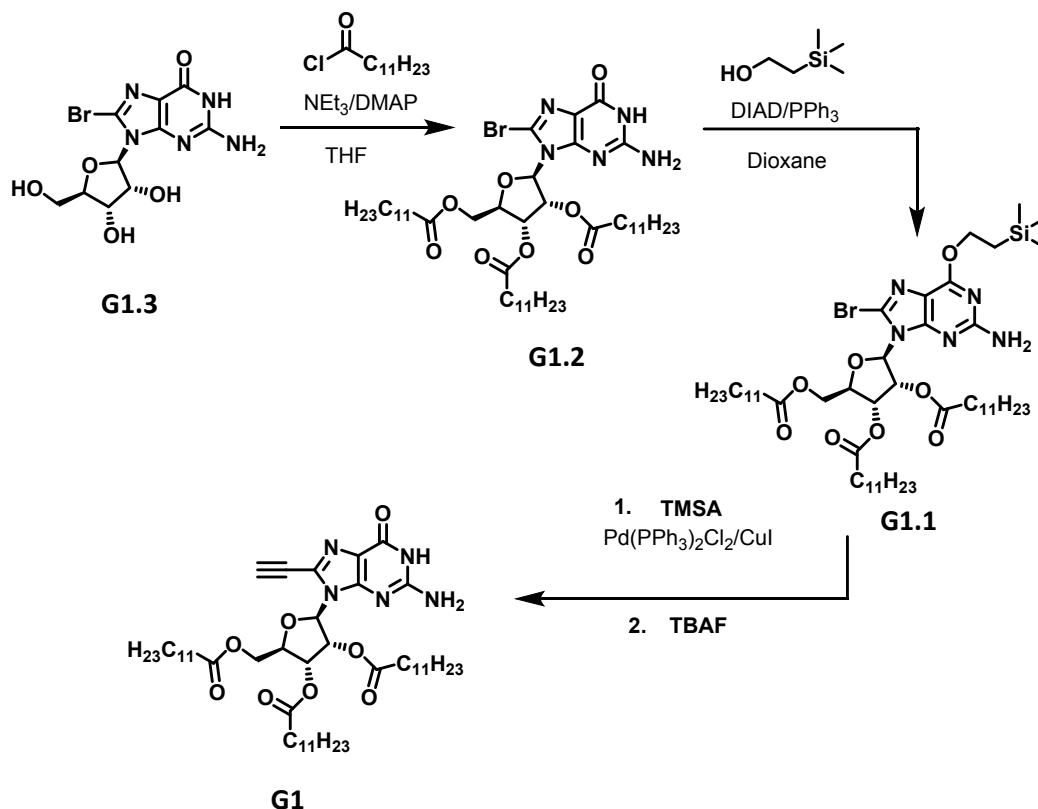
C1. In a round-bottomed flask equipped with a magnetic stirrer, **C1.1**. (1.39 mmol, 1.23 g) was placed and dissolved with 40 mL of THF/MeOH (1:1). Then KF (2.08 mmol, 121 mg) was slowly added at room temperature, and the mixture was stirred until reaction completion (1 h). The precipitation of KF was promoted by the addition of toluene. The mixture was filtered over celite and the solvent was evaporated at reduced pressure. **C1** was obtained as a brown oil (0.89 g, 77 %) by chromatography on silica gel purification eluted with CHCl₃/MeOH (50:1).

¹H NMR (300 MHz, CDCl₃) δ(ppm) = 8.42 (s, 1H, NH^{4c}), 7.90 (s, 1H, H^{6c}), 6.05 (d, *J* = 3.5 Hz, 1H, H^{1c}), 5.94 (s, 1H, NH^{4c}), 5.36 (dd, *J* = 5.5 Hz, 3.5 Hz, 1H, H^{2c}), 5.27 (t, *J* = 5.5 Hz, 1H, H^{4c}), 4.33 (s, 3H, CH₂^{5c}, H^{3c}), 3.33 (s, 1H, H^b), 2.45-2.21 (m, 6H, -OCOCH₂-), 1.68-1.48 (m, 6H, OCOCH₂CH₂-), 1.23 (d, *J* = 6.0 Hz, 48H, OCOC₂H₄-(CH₂)_{*n*}-) 0.84 (t, *J* = 6.0 Hz, 9H, -CH₃).

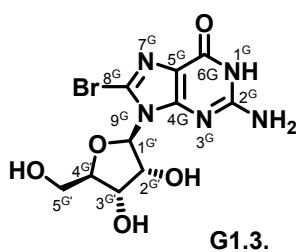
¹³C NMR (75 MHz, CDCl₃) δ(ppm) = 173.0, 172.2, 172.0, 164.7, 153.7, 144.1, 90.9, 88.6, 83.9, 79.6, 74.9, 73.7, 69.2, 62.3, 34.1, 33.8, 31.9, 29.6, 29.5, 29.3, 29.2, 29.1, 24.8, 24.7, 22.7, 14.1.

HRMS (FAB+): Calculated for C₄₇H₇₉N₃O₈Na: 836.5759 [M+Na]⁺. Found: 836.5763.

Synthetic procedures and characterization data for G1.



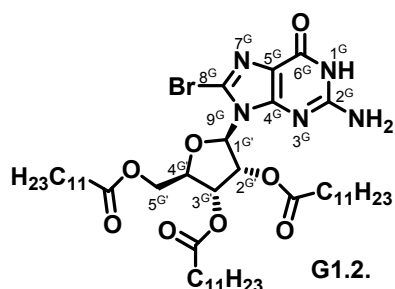
Scheme S3. Synthetic route to G1.



G1.3.^{S6} Commercial guanosine (35 mmol, 10 g) was dissolved in a round-bottomed flask with 166 mL of mixture MeCN/H₂O (4:1) and NBS (52.9 mmol, 9.40 g) was added over a period of 30 min. The reaction was completed in 1h. The mixture was then filtered through a filter paper and the filtrate was washed with cold acetone. **G1.3.** was obtained as a white solid (11.40 g, 90 %).

¹H NMR (300 MHz, DMSO) δ (ppm) = 10.81 (s, 1H, NH^{1G}), 6.49 (s, 2H, NH₂^{2G}), 5.69 (d, *J* = 6.0 Hz, 1H, H^{1G}), 5.44 (d, *J* = 6.0 Hz, 1H, H^{2G}), 5.08 (d, *J* = 5.0 Hz, 1H, H^{3G}), 5.05-4.97 (m, 1H, -OH^{3G}), 4.95-4.86 (m, 1H, H^{4G}), 4.14 (q, *J* = 5.0 Hz, 1H, -OH^{2G}), 3.90-3.82 (m, 1H, -OH^{5G}), 3.66 (dt, *J* = 11.0, 5.0 Hz, 1H, CH^{5G}), 3.52 (dt, *J* = 12.0, 6.0 Hz, 1H, CH^{5G}).

¹³C NMR (75 MHz, DMSO) δ (ppm) = 155.4, 153.4, 121.1, 89.6, 85.8, 70.5, 70.2, 62.0



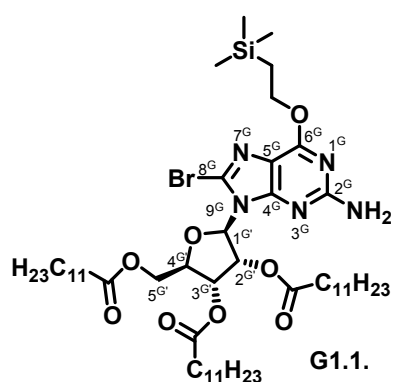
G1.2.^{S7,S8} In a 500 mL round-bottomed flask, equipped with a magnetic stirrer, **G1.3.** (11.0 mmol, 4 g) and DMAP (2.2 mmol, 267 mg) were placed. Dry DMF (400 mL) was added and the mixture was stirred at room temperature under argon until the solid was dissolved. Then NEt₃ (17 mmol, 2.4 mL) and lauryl chloride (33.0 mmol, 7.62 mL) were added. The resulting mixture was stirred at 130 °C until

G1.3. was consumed. Afterwards, MeOH (7 mL) was added and the mixture was stirred during 15 minutes. The solvent was eliminated under reduced pressure and the solid was directly purified by chromatography on silica gel eluted with CHCl₃/MeOH (60:1). **G1.2.** was obtained as a white solid (6.80 g, 68 %).

¹H NMR (300 MHz, CDCl₃) δ(ppm) = 11.94 (s, 1H, NH^{1G}), 6.30 (s, 2H, NH₂^{2G}), 5.94 (s, 2H, H^{1G;2G}), 4.41 (d, *J* = 44.5 Hz, 4H, H^{3G;4G}, CH₂^{5G}), 2.58-2.04 (m, 6H, -OCOCH₂-) 1.77-1.09 (m, 54H, -CH₂-), 0.8 (m, 9H, -CH₃).

¹³C NMR (75 MHz, CDCl₃) δ (ppm) = 179.2, 173.6, 172.3, 172.1, 172.0, 158.4, 157.7, 153.4, 152.4, 121.9, 117.8, 116.7, 88.4, 79.7, 72.0, 70.3, 62.9, 34.1, 34.0, 33.9, 33.8, 31.9, 29.6, 29.4, 29.3, 29.3, 29.1, 25.1, 24.8, 22.7, 14.1.

HRMS (MALDI): Calculated for C₄₆H₇₈BrN₅NaO₈: 932.4877 [M+Na]⁺. Found: 932.4917



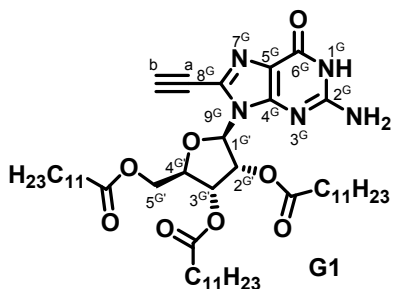
G1.1. In a 250-mL round-bottomed flask, equipped with a magnetic stirrer, **G1.2.** (7.48 mmol, 6.80 g), PPh₃ (28.61 mmol, 7.50 g) and DIAD (6.27 mmol, 1.24 mL) were placed. Dry dioxane (140 mL) was added and the mixture was stirred at room temperature under argon atmosphere until the solid was dissolved. Then 2-trimethylsilylethanol was added dropwise (11.96 mmol, 1.72 mL) and the mixture was stirred at room temperature during 12 h. Finally, the solvent was eliminated under reduced pressure and the oil obtained was purified by chromatography on silica gel eluted with Hexane/AcOEt (10:1) to

yield a brown solid (5.97 g, 79 %).

¹H NMR (300 MHz, CDCl₃) δ(ppm) = 6.28 (dd, *J* = 5.5, 4.0 Hz, 1H, H^{1G}), 6.09 (t, *J* = 5.5 Hz, 1H, H^{2G}), 5.99 (d, *J* = 4.0 Hz, 1H, H^{4G}), 4.95 (s, 2H, NH₂^{2G}), 4.59-4.49 (m, 3H, H^{3G}, CH₂^{5G}), 4.41-4.30 (m, 2H, -OCH₂CH₂Si), 2.40-2.30 (m, 4H, OCOCH₂-), 2.29-2.14 (m, 2H, C^{5G}OCOCH₂-), 1.71-1.46 (m, 2H, OCH₂CH₂Si), 1.40-1.10 (m, 54 H, -CH₂-), 0.94-0.62 (m, 9H, -CH₃), 0.08 (s, 9H, -Si(CH₃)₃).

¹³C NMR (75 MHz, CDCl₃) δ (ppm) = 175.0, 173.8, 173.6, 161.9, 160.5, 155.2, 130.0, 129.8, 125.9, 117.6, 89.9, 81.1, 73.5, 71.8, 66.6, 64.2, 35.4, 35.4, 35.3, 33.3, 31.1, 31.1, 31.0, 30.9, 30.9, 30.8, 30.7, 30.7, 30.6, 30.5, 26.3, 26.3, 26.2, 24.1, 19.0, 15.5, 0.3, 0.0, -0.3.

MS (FAB+): found: 1010.3 [M+H]⁺.



G1. G1.1. (5.9 mmol, 5.97 g), Pd(PPh₃)₂Cl₂ (0.06 mmol, 46 mg) and CuI (0.02 mmol, 8.0 mg) were mixed in deoxygenated THF/NEt₃ (4:1, 80 mL) by *freeze-pump-thaw* cycles. TMSA (10 mmol, 1.20 g) was added dropwise over the solution and the mixture was then stirred at 40 °C during 24 h until **G1.1** is completely consumed. The solution was filtered over celite and evaporated. The crude was directly deprotected by slowly addition of TBAF·3H₂O (8 mmol, 2.52 g) over the crude in

THF (80 mL). After approximately 1 h the solvent was evaporated and the brown oil was purified by

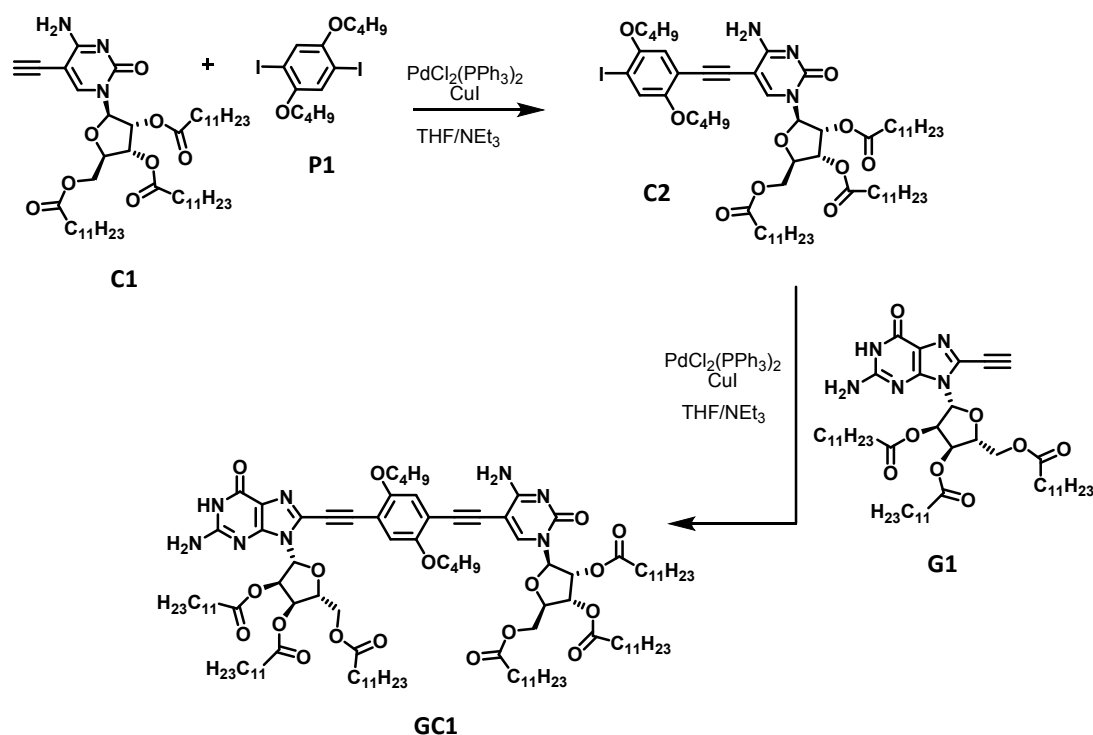
chromatography on silica gel eluted with $\text{CHCl}_3/\text{MeOH}$ (20:1). **G1** was obtained as a brown solid (3.07 g, 61 %).

^1H NMR (300 MHz, CDCl_3) δ (ppm) = 12.12 (s, 1H, $\text{NH}^{1\text{G}}$), 6.28 (s, 2H, $\text{NH}_2^{2\text{G}}$), 6.15-5.96 (m, 2H, $\text{H}^{1\text{G}}, 2\text{G}$), 5.93-5.82 (m, 1H, $\text{H}^{4\text{G}}$), 4.53-4.35 (m, 1H, $\text{H}^{3\text{G}}$), 4.38-4.21 (m, 2H, $\text{CH}_2^{5\text{G}}$), 3.37 (s, 1H, H^b), 2.40-2.15 (m, 6H, OCOCH_2), 1.65-1.41 (m, 6H, $\text{OCOCH}_2\text{CH}_2$), 1.32-1.01 (m, 48H, $-\text{CH}_2-$), 0.88-0.69 (m, 9H, $-\text{CH}_3$).

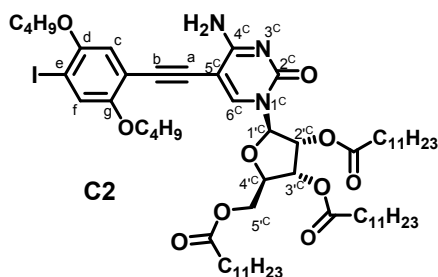
^{13}C NMR (75 MHz, CDCl_3) δ (ppm) = 172.6, 171.3, 171.0, 157.5, 153.0, 150.1, 129.2, 116.5, 86.3, 82.2, 78.7, 76.2, 71.5, 69.4, 62.0, 33.0, 32.9, 32.8, 30.9, 28.7, 28.6, 28.6, 28.5, 28.5, 28.4, 28.3, 28.3, 28.3, 28.2, 28.1, 25.9, 23.8, 21.7, 13.1.

MS (MALDI): found: 876.6 $[\text{M}+\text{Na}]^+$.

Synthesis of Monomer GC1.



Scheme S4. Synthetic route to **GC1**.



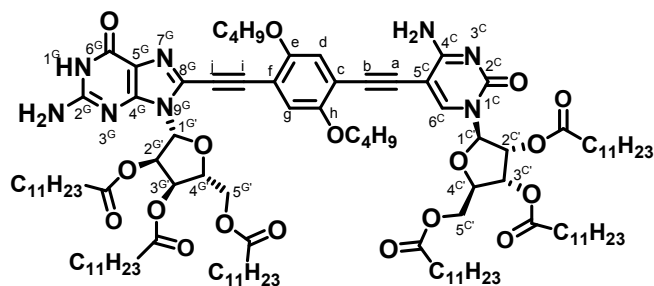
C2 was prepared according to a standard procedure for the Sonogashira coupling reaction between the ethynyl-nucleobase **C1** and **P1**. A dry THF/NEt₃ (4:1) mixture (8 mL) was subjected to deoxygenation by three *freeze-pump-thaw* cycles with argon and poured over **C1** (0.122 mmol, 83 mg), **P1** (1.22 mmol, 578.4 mg), Pd(PPh₃)₂Cl₂ (0.003 mmol, 1.88 mg,) and CuI (0.0014 mmol, 0.25 mg). The mixture was stirred under argon for 12 h at room

temperature. Once completed, the mixture was filtered over a celite plug and the solvent was evaporated under reduced pressure. The product was purified by column chromatography on silica gel eluted with CHCl₃/MeOH (50:1), affording **C2** as a yellow oil (77 mg, 82 %). The excess of **P1** was recovered.

¹H RMN (300 MHz, CDCl₃) δ(ppm) = 7.90 (s, 1H, *H*^{6c}), 7.30 (s, 1H, *H*^c), 6.76 (s, 1H, *NH*^{4c}), 6.30 (s, 1H, *H*^f), 6.19 (d, *J* = 4.0 Hz, 1H, *H*^{1c}), 5.42-5.36 (m, 1H, *H*^{2c}), 5.36-5.19 (m, 1H, *H*^{4c}), 4.38 (s, 3H, *CH*₂^{5c}, *H*^{3c}), 3.97 (dt, *J* = 13.0, 6.5 Hz, 4H, *C*^{d,g}-OCH₂), 2.46 (t, *J* = 7.5 Hz, 2H, *C*^{3c}-OCOCH₂-), 2.39-2.23 (m, 4H, *C*^{2c}-OCOCH₂- *C*^{5c}-OCOCH₂-), 1.89-1.71 (m, 4H, *C*^{d,g}-OCH₂CH₂-), 1.71-1.44 (m, 10H, *C*^{d,g}-OC₂H₄CH₂CH₃, OCOC₂H₄CH₂-), 1.37-1.09 (m, 48H, -CH₂-), 0.98 (q, *J* = 7.0 Hz, 6H, *C*^{d,g}-OC₃H₆-CH₃), 0.87 (t, *J* = 6.5 Hz, 9H, OCOC₁₀H₂₀-CH₃).

¹³C NMR (75 MHz, CDCl₃) δ(ppm) = 173.1, 172.3, 172.2, 164.2, 154.1, 153.8, 151.9, 141.8, 122.9, 114.5, 111.8, 93.0, 92.2, 88.4, 88.3, 85.0, 79.7, 77.2, 73.7, 69.9, 69.4, 69.2, 62.6, 34.2, 33.9, 31.9, 31.3, 31.2, 29.6, 29.5, 29.4, 29.3, 29.2, 29.1, 24.9, 24.7, 22.7, 19.3, 19.1, 14.1, 13.8.

HRMS (MALDI): Calculated for C₆₁H₉₉IN₃O₁₀: 1160.6297 [M+H]⁺. Found: 1160.6406.



GC1

GC1 was prepared according to a standard procedure for the Sonogashira coupling reaction between the ethynyl-nucleobase **G1** and **C2**. A dry THF/ NEt_3 (4:1) mixture (3 mL) was subjected to deoxygenation by three freeze-pump-thaw cycles with argon and poured over **G1** (0.066 mmol, 56.7 mg), **C2** (0.06 mmol, 70 mg), $\text{Pd}(\text{PPh}_3)_2\text{Cl}_2$ (0.0012

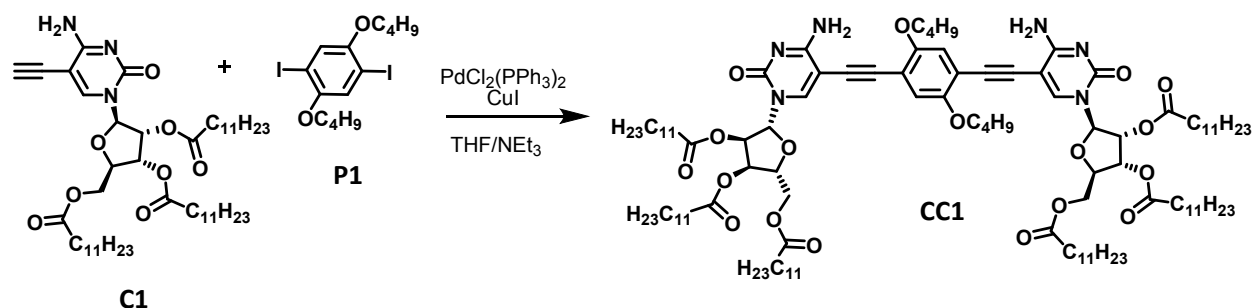
mmol, 0.84 mg) and CuI (0.002 mmol, 0.4 mg). The mixture was stirred under argon for 12 h at 40 °C. Once completed, the mixture was filtered over a celite plug and the solvent was evaporated under reduced pressure. The product was purified by column chromatography on silica gel eluted with $\text{CHCl}_3/\text{MeOH}$ (40:1), affording **GC1** as a yellow solid (50 mg, 44 %).

^1H RMN (300 MHz, $\text{THF-}d_8$) δ (ppm) = 13.26 (s, 1H, $\text{NH}^{1\text{G}}$), 10.09 (s, 1H, $\text{NH}^{4\text{C}}$), 7.96 (s, 1H, $\text{H}^{6\text{C}}$), 7.09 (s, 1H, H^{d}), 6.90 (s, 1H, H^{g}), 6.55 (s, 1H, $\text{H}^{1\text{G}}$), 6.21 (s, 1H, $\text{H}^{1\text{C}}$), 6.18-6.16 (m, 2H, $\text{H}^{2\text{C}}, 4\text{C}$), 6.06-6.02 (m, 1H, $\text{H}^{2\text{G}}$), 5.87-5.82 (m, 1H, $\text{H}^{4\text{G}}$), 5.67-5.61 (m, 1H, $\text{H}^{3\text{G}}$), 5.50-5.43 (m, 1H, $\text{H}^{3\text{C}}$), 4.91 (s, 1H, $\text{NH}^{2\text{G}}$), 4.68- 4.58 (m, 1H, $\text{NH}^{2\text{G}}$), 4.57-3.87 (m, 8H, $\text{CH}_2^{5\text{C}}, \text{CH}_2^{5\text{G}}, \text{C}^{\text{e}}\text{-OCH}_2\text{-}, \text{C}^{\text{h}}\text{-OCH}_2\text{-}$), 2.36-2.02 (m, 18H, OCOCH_2), 1.78-0.92 (m, 116H, $\text{-CH}_2\text{-}$), 0.89-0.60 (m, 18H, $\text{OCOC}_{10}\text{H}_{20}\text{-CH}_3$).

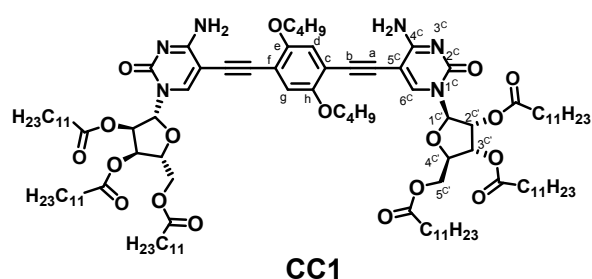
^{13}C NMR (76 MHz, CDCl_3) δ (ppm) = 172.6, 171.3, 171.0, 157.5, 153.0, 150.1, 129.2, 116.5, 86.3, 82.2, 78.7, 76.2, 71.5, 69.4, 62.0, 33.0, 32.9, 32.8, 30.9, 28.7, 28.6, 28.6, 28.5, 28.5, 28.4, 28.3, 28.3, 28.2, 28.1, 25.9, 23.8, 23.8, 21.7, 13.1.

MS (MALDI): found: 1909.2 $[\text{M}+\text{H}+\text{Na}]^+$.

Synthesis of Monomer CC1.



Scheme S5. Synthetic route to **CC1**.



CC1 was prepared according to a standard procedure for the Sonogashira coupling reaction between the ethynyl-nucleobase **C1** and **P1**. A dry THF/ NEt_3 (4:1) mixture (3 mL) was subjected to deoxygenation by three *freeze-pump-thaw* cycles with argon and poured over **C1** (0.614 mmol, 500 mg), **P1** (0.430 mmol, 204 mg), $\text{Pd}(\text{PPh}_3)_2\text{Cl}_2$ (0.013 mmol, 9.5 mg), and CuI (0.002 mmol, 1.3 mg). The mixture was stirred under argon for 12 h at 40 °C. Once completed, the mixture was filtered over a celite plug and the solvent was evaporated under reduced pressure. The product was purified by column chromatography on silica gel eluted with $\text{CHCl}_3/\text{MeOH}$ (40:1), affording **CC1** as a yellow solid (202 mg, 35 %).

$^1\text{H RMN}$ (300 MHz, CDCl_3) δ (ppm) = 7.88 (s, 2H, H^{6c}), 6.87 (s, 2H, $H^{g,d}$), 6.40 (s, 2H, NH^{4c}), 6.33 (s, 2H, NH^{4c}), 6.18 (d, $J = 4.0$ Hz, 2H, H^{1c}), 5.47-5.37 (m, 2H, H^{2c}), 5.33 (dd, $J = 6.5, 4.0$ Hz, 2H, H^{4c}), 4.38 (s, 6H, CH_2^{5c} , H^{3c}), 4.01 (t, $J = 6.5$ Hz, 4H, $\text{C}^{e,h}\text{-OCH}_2$), 2.46 (t, $J = 7.5$ Hz, 4H, CH_2^{5c}), 2.41-2.25 (m, 12H, OCOCH_2^-), 1.87-1.72 (m, 4H, $\text{C}^{e,h}\text{-OCH}_2\text{CH}_2^-$), 1.72-1.40 (m, 12H, $\text{OCOCH}_2\text{CH}_2^-$), 1.39-1.11 (m, 96H, CH_2), 0.98 (t, $J = 7.5$ Hz, 6H, $\text{OC}_3\text{H}_6\text{-CH}_3$), 0.87 (t, $J = 6.3$ Hz, 18H, $\text{OCOC}_{10}\text{H}_{20}\text{-CH}_3$).

$^{13}\text{C NMR}$ (76 MHz, CDCl_3) δ (ppm) = 173.1, 172.3, 172.2, 164.3, 153.8, 153.4, 142.0, 114.4, 112.7, 93.2, 92.0, 88.5, 86.3, 79.7, 77.2, 73.7, 69.5, 69.1, 62.7, 34.2, 33.9, 31.9, 31.9, 31.3, 29.6, 29.5, 29.4, 29.3, 29.2, 29.1, 24.9, 24.7, 22.7, 19.2, 14.1, 13.8.

MS (MALDI): found: 1869.2 $[\text{M}+\text{Na}]^+$.

S3. Preliminary study of the self-assembly behavior of GC1

Prior to their combination with CNTs we wanted to confirm that the new **GC1** monomer followed a similar self-assembly process to the one already reported by us with closely related dinucleosides.^{S1} 10^{-2} – 10^{-5} M solutions of **GC1** in CDCl_3 or $\text{CDCl}_2\text{CDCl}_2$ displayed ^1H NMR spectra that are characteristic of quantitative G-C H-bonding, as confirmed by NOESY NMR (Figure S1a), with G-H¹ and C-H¹ H-bonded protons appearing around 13.4 ppm and 10.0 ppm, respectively (see as an example the bottom spectrum in Figure S1b). In contrast to G-C supramolecular polymers or 1:1 mixtures of G and C mononucleosides, the shape and position of these two H-bonded signals do not change significantly with concentration, temperature or small solvent composition variations. This finding is already an indication that an especially stabilized H-bonded species is present in solution, whose size, estimated by DOSY NMR and ESI Q-TOF experiments in our previous work,^{S1} matches the one expected for a cyclic tetramer. Further corroboration was obtained by adding increasing amounts of a polar solvent that can compete for the H-bonding sites, like DMSO or DMF, which results in monomer dissociation. The ^1H NMR spectra recorded along these titrations (Figure S1b) is again markedly different to the one that would be expected for a H-bonded supramolecular polymerization and reveal a strong all-or-nothing behavior. Only monomer and cyclic tetramer species are detected in slow exchange at the NMR timescale, which is in agreement with the formation of a thermodynamically and kinetically stable ring species with high chelate cooperativity, as proven in our previous work.^{S1}

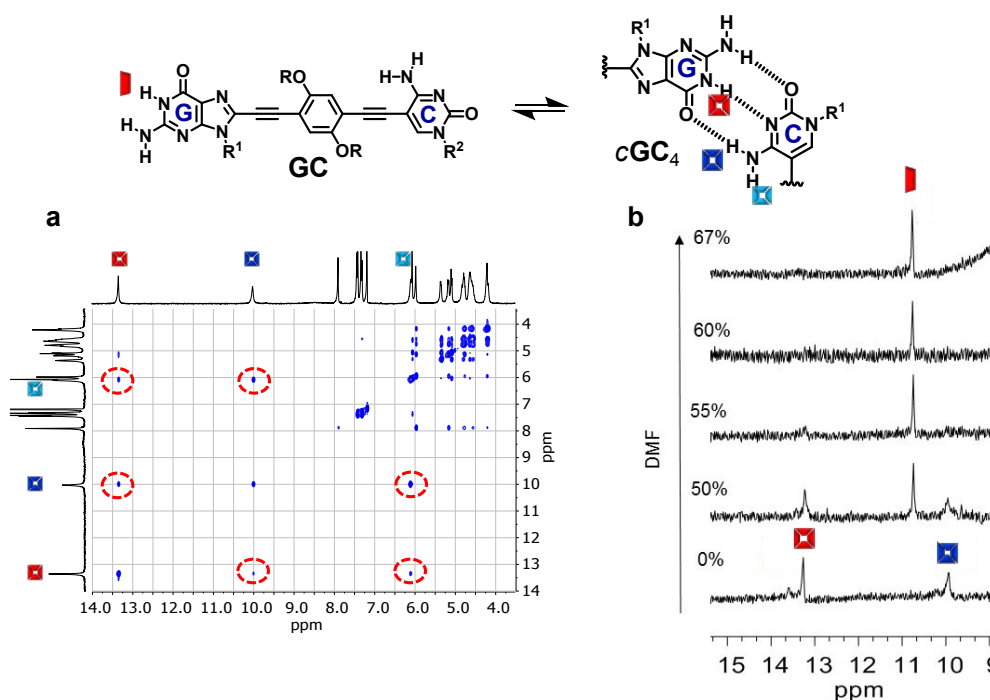


Figure S1. (a) Region of the NOESY NMR spectrum of **GC** in CDCl_3 ($C = 1.0 \times 10^{-2}$ M, $T = 298$ K), showing cross-peaks between the H-bonded G-amide and C-amine proton signals. (b) Evolution of the downfield region of the ^1H NMR spectra of **GC1** as the volume fraction of DMF- D_7 is increased in CDCl_3 -DMF- D_7 mixtures at $C = 3.0 \cdot 10^{-3}$ M and $T = 298$ K. The cyclic tetramer in CDCl_3 , showing the H-bonded G-amide (at ca. 13.4 ppm) and C-amine (at ca. 10.0 ppm) proton signals, is progressively dissociated into monomer species, that show a G-amide peak at ca. 10.8 ppm, as the DMF content is increased. Please note that the shape and position of each signal do not change significantly along these titrations, suggesting an equilibrium between 2 species (monomer and tetramer) in slow exchange at the NMR timescale, as determined in our previous work.^{S1}

The cyclotetramerization process can also be monitored by more sensitive techniques like absorption, emission and circular dichroism (CD) spectroscopy. **GC1** monomers display emission maxima at 421 and 445 nm and null CD signals. Compared to these features, **GC1** nanorings are spectroscopically characterized by red-shifted and low intensity emission maxima at 503 nm, and by the presence of a characteristic negative Cotton effect with maxima at 339 and 386 and a minimum at 428 nm, which is originated by cyclic H-bonding assembly.^{S1} As in our previous work, a series of experiments performed as a function of sample concentration allowed us to estimate the degree of cyclotetramerization, that is, the molar fraction of **GC1** molecules assembled as cyclic tetramers in solution. In the case of the CD experiments, this is done by integrating the area of the CD spectra. For the emission experiments, this is carried out by analyzing the shape of the emission spectra. From our own experience in this and previous studies,^{S1} the best way to do this is to calculate the ratio between emission intensity above and below a chosen intermediate wavelength and correlate these values to those obtained with pure cyclic tetramer and pure monomer.

Altogether, NMR and optical spectroscopy experiments indicate that **GC1** cyclic tetramers are formed close to quantitatively in apolar chlorinated solvents at room temperature within the 10^{-2} - 10^{-4} concentration range. At lower concentrations or upon addition of polar solvents they dissociate gradually into monomeric species, a process that can be monitored spectroscopically giving rise to sigmoidal curves that can be fitted to a cyclotetramerization process.

S4. Characterization of the pristine (6,5)-enriched SWNTs

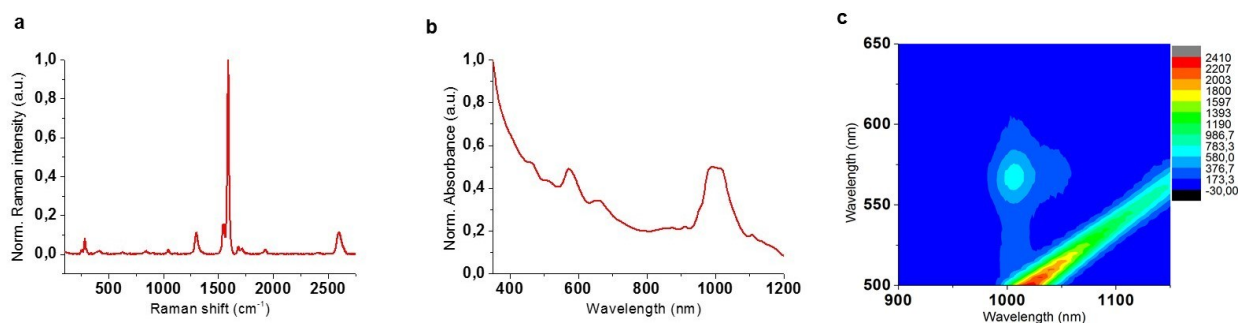


Figure S2. (a) Raman spectra ($\lambda_{\text{exc}} = 633 \text{ nm}$), (b) UV-vis-NIR spectra (D_2O , 1 % SDS, 298 K), (c) PLE intensity map (D_2O , 1 % SDS, 298 K) of pristine (6,5)-enriched SWNTs. All spectroscopic data support a sample which is nearly exclusively semiconducting, with (6,5) as the main chirality present, as stated by the provider.

S5. Computational Details

All theoretical calculations were carried out within the density functional theory (DFT) approach by using the C.01 revision of the Gaussian 09 program package.^{S9} Considering the two moieties of the final composites: (6,5)-SWCNT and **GC1** tetrameric ring we need to divide the modeling process in two stages. First, we investigate the stabilization of the **GC1** tetrameric ring by using the Coulomb-attenuated hybrid exchange-correlation functional (CAM-B3LYP) functional. This functional was developed by Yanai *et al.*^{S10} which includes the Hartree-Fock and the Becke exchanges as a variable ratio depending of the intermolecular distance. It has been demonstrated that this method gives an improved description of long-range interactions and really good agreements between the experimental and theoretical circular dichroism spectra.^{S11-S13} In the present study, we employed the CAM-B3LYP functional for the investigation of the stabilization and chiroptical properties of the **GC1** tetrameric ring. Electronic excitation energies of the **GC1** tetrameric ring were obtained by using the time-dependent DFT (TD-DFT) formalism^{S14,S15} for which up to the 20 low-lying energy states were considered. Additionally, the **GC1** tetrameric ring was simplified by substituting $-\text{OCC}_{11}\text{H}_{23}$ chains attached to the desoxyribosees by $-\text{OH}$. Also, the $-\text{OC}_4\text{H}_9$ chains attached to the benzene in the connector groups were reduced to $-\text{OCH}_3$, in order to reduce the computational cost. Secondly, the binding energy of (6,5)SWCNT-**GC1** composites were studied using the long-range corrected B97D density functional, which are able to incorporate the dispersion effects by means of a pair-wise London-type potential. The B97D^{S16} density functional has emerged as a robust and powerful density functional able to provide accurate structures in large supramolecular aggregates, specifically composites with carbon nanotubes.^{S17-S19} The Pople's 3-21G* basis set^{S20} was employed in both cases to reduce the computational cost.

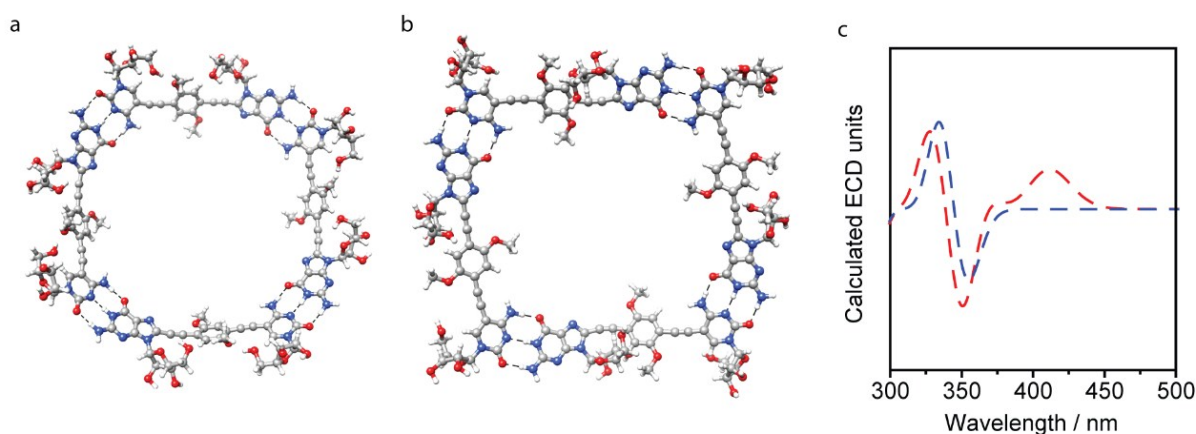


Figure S3. Optimized structure of (a) C_4 -symmetric and (b) non-symmetric **GC1** tetrameric ring. (c) Circular dichroism spectra of both conformers. Color code: blue: C_4 -symmetric and red: non symmetric **GC1** tetrameric ring.

$$E_{int} = E_{(6,5)SWCNT - GC1 \text{ composite}} - (E_{(6,5)SWCNT} - E_{GC1 \text{ tetrameric ring}})$$

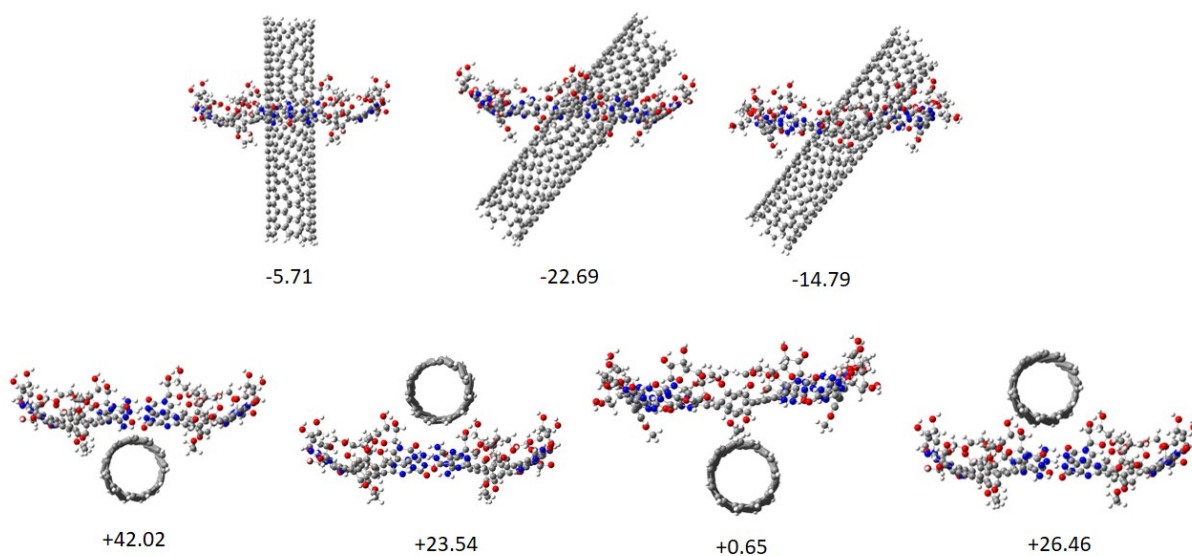


Figure S4. Different configurations of the (6,5)SWCNT-GC1 composite. Definition of interaction energy (E_{int}) and energy parameters (Kcal mol⁻¹) for the different configuration.

S6. Characterization of the CNT-GC1 conjugates by HR-TEM

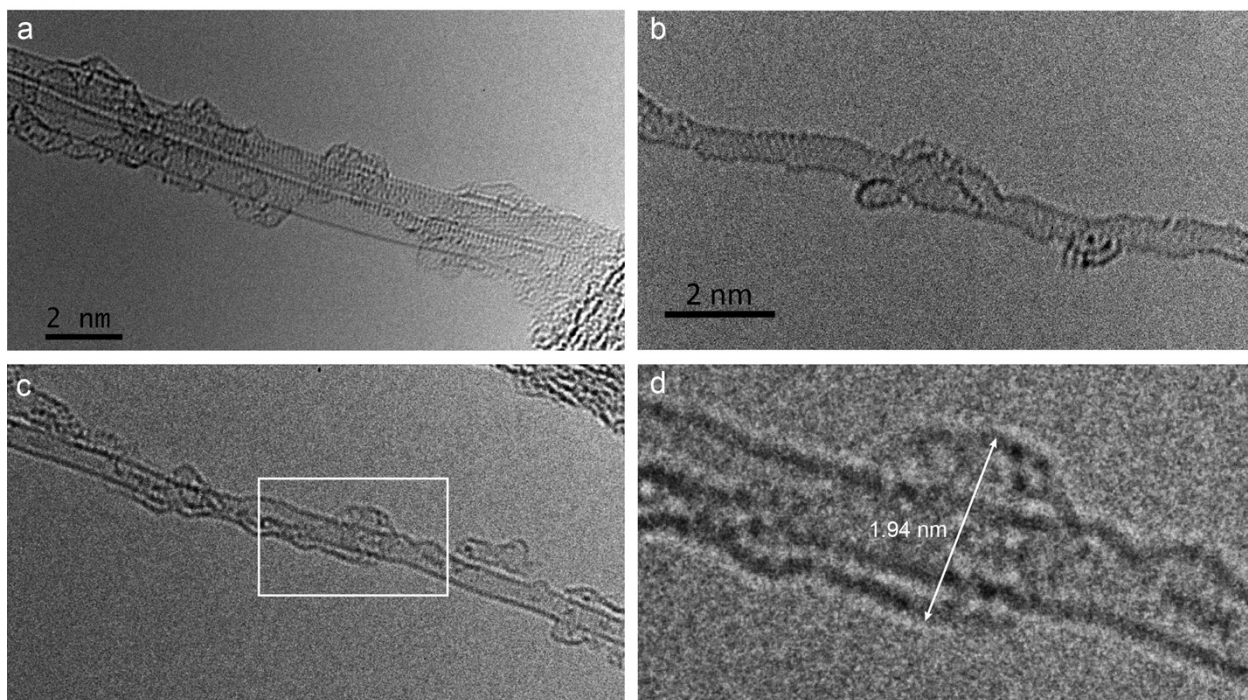


Figure S5. Representative aberration corrected HR-TEM images of SWCNT-**GC1** conjugates. Note that the walls of the SWNTs are heavily functionalized (a) but the addends, and even the walls of the SWNT are quickly damaged (b) under the e-beam. In some images, structures that could correspond to the **GC1** macrocycles are still visible (c and d).

S7. Dilution experiments monitored by fluorescence spectroscopy

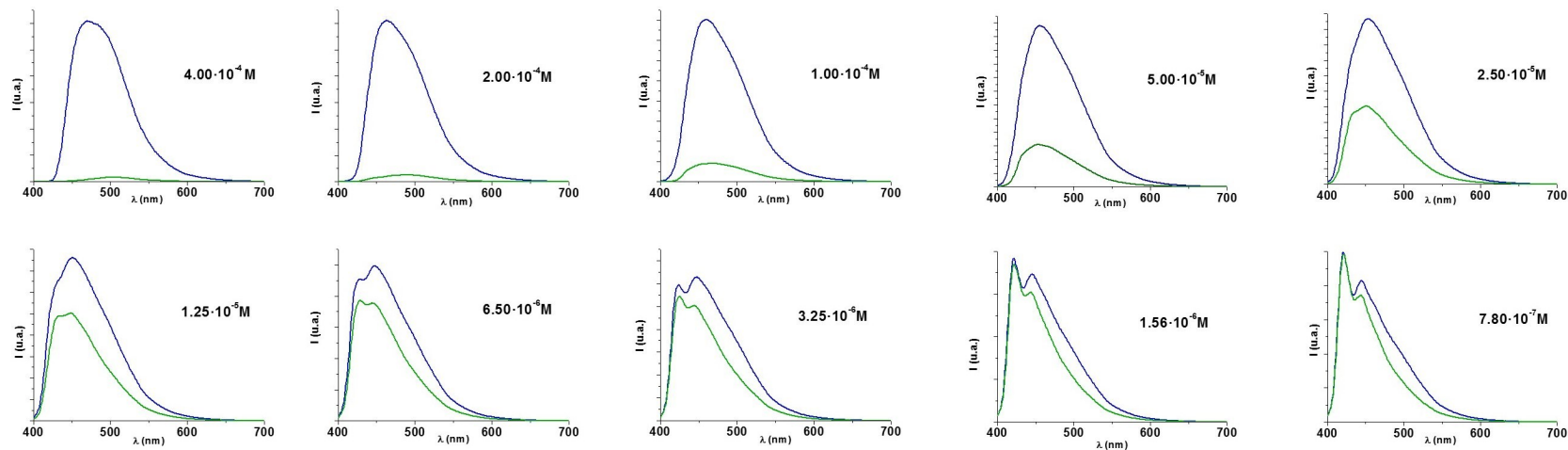


Figure S6A. Selected emission spectra ($\lambda_{\text{exc}} = 380 \text{ nm}$) of **GC1** at different concentrations in CHCl_3 and in the absence (I_{GC}) (blue line) or presence ($I_{\text{GC-CNT}}$) of (6,5)SWCNTs (green line).

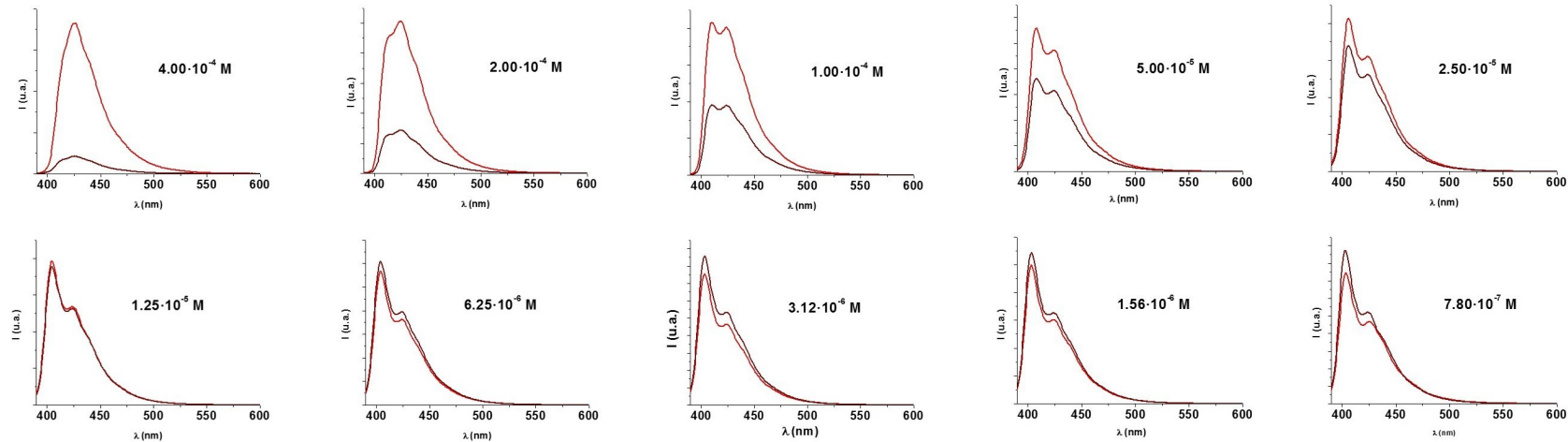


Figure S6B. Selected emission spectra ($\lambda_{\text{exc}} = 380 \text{ nm}$) of **CC1** at different concentrations in CHCl_3 and in the absence (I_{CC}) (red line) or presence ($I_{\text{CC-CNT}}$) of (6,5)SWCNTs (brown line).

S8. References

- S1. C. Montoro-García, J. Camacho-García, A. M. López-Pérez, N. Bilbao, S. Romero-Pérez, M. J. Mayoral and D. González-Rodríguez, *Angew. Chem. Int. Ed.*, 2015, **54**, 6780-6784.
- S2. C. Montoro-García, N. Bilbao, I. M. Tsagri, C. F. Guerra and D. González-Rodríguez, *Manuscript in preparation*.
- S3. L. Zibiao and T. Beng Hoon, *Dyes and Pigments*, 2012, **94**, 88-98.
- S4. T. Shiraki, S. Haraguchi, Y. Tsuchiya and S. Shinkai, *Chem. Asian J.*, 2009, **4**, 1434-1441.
- S5. M. J. Plater, J. P. Sinclair, S. Aiken, T. Gelbrich and M. B. Hursthouse, *Tetrahedron*, 2004, **60**, 6385-6394.
- S6. D. González-Rodríguez, P. G. A. Janssen, R. Martín-Rapún, I. De Cat, S. De Feyter, A. P. H. J. Schenning and E. W. Meijer, *J. Am. Chem. Soc.*, 2010, **132**, 4710-4719.
- S7. B. Zhang, Z. Cui and L. Sun, *Org. Lett.*, 2001, **3**, 275-2787.
- S8. Y. Xu, H. Jin, Z. Yang and L. Zhang, *Tetrahedron*, 2009, **65**, 5228-5239.
- S9. M. J. Frisch, G. W. Trucks, H. B. Schlegel, G. E. Scuseria, M. A. Robb, J. R. Cheeseman, G. Scalmani, V. Barone, B. Mennucci, G. A. Petersson, H. Nakatsuji, M. Caricato, X. Li, H. P. Hratchian, A. F. Izmaylov, J. Bloino, G. Zheng, J. L. Sonnenberg, M. Hada, M. Ehara, K. Toyota, R. Fukuda, J. Hasegawa, M. Ishida, T. Nakajima, Y. Honda, O. Kitao, H. Nakai, T. Vreven, J. A. Montgomery, J. E., Peralta, F. Ogliaro, M. Bearpark, J. J. Heyd, E. Brothers, K. N. Kudin, V. N. Staroverov, R. Kobayashi, J. Normand, K. Raghavachari, A. Rendell, J. C. Burant, S. S. Iyengar, J. Tomasi, M. Cossi, N. Rega, J. M. Millam, M. Klene, J. E. Knox, J. B. Cross, V. Bakken, C. Adamo, J. Jaramillo, R. Gomperts, R. E. Stratmann, O. Yazyev, A. J. Austin, R. Cammi, C. Pomelli, J. W. Ochterski, R. L. Martin, K. Morokuma, V. G. Zakrzewski, G. A. Voth, P. Salvador, J. J. Dannenberg, S. Dapprich, A. D. Daniels, O. Farkas, J. B. Foresman, J. V. Ortiz, J. Cioslowski and D. J. Fox, *Wallingford CT*, 2009.
- S10. T. Yanai, D. P. Tew and N. C. Handy, *Chem. Phys. Lett.*, 2004, **393**, 51-57.
- S11. B. Nieto-Ortega, J. Casado, J. T. L. Navarrete, G. Hennrich and F. J. Ramírez, *J. Chem. Theory Comput.*, 2011, **7**, 3314-3322.
- S12. F. Di Meo, M. N. Pedersen, J. Rubio-Magnieto, M. Surin, M. Linares and P. Norman, *J. Phys. Chem. Lett.*, 2015, **6**, 355-359.
- S13. P. Rivera-Fuentes, B. Nieto-Ortega, W. B. Schweizer, J. T. L. Navarrete, J. Casado and D. Diederich, *Chem. Eur. J.*, 2011, **17**, 3876-3885.
- S14. E. Runge and E. K. U. Gross, *Phys. Rev. Lett.*, 1984, **52**, 997-1000.
- S15. E. K. U. Gross and W. Kohn, *Advances in Quantum Chemistry*, (Ed.: L. Per-Olov), Academic Press, 1990, **21**, 255-291.
- S16. S. Grimme, *J. Comput. Chem.*, 2006, **27**, 1787-1799.
- S17. S. Aljohani, A. I. Alrawashdeh, M. Z. H. Khan, Y. Zhao and J. B. Lagowski, *J. Phys. Chem. C*, 2017, **121**, 4692-4702.
- S18. B. B. Shirvani, M. B., Shirvani, J. Beheshtian and N. L. Hadipour, *J. Iran. Chem. Soc.*, 2011, **8**, S110-S118.
- S19. A. Joshi and C. N. Ramachandran, *Phys. Chem. Chem. Phys.*, 2016, **18**, 14040-14045.
- S20. J. S. Binkley, J. A., Pople and W. J. Hehre, *J. Am. Chem. Soc.*, 1980, **102**, 939-947.